NMR Imaging for Core Flood Testing

- by M. P. Enwere and J. S. Archer; Imperial College, London.

Abstract: Use of nuclear magnetic resonance (NMR) imaging to measure one-dimensional (1-D) saturation distributions along the direction of flow at various flood stages is presented. Dynamically measured saturation profiles are used in conjunction with capillary pressure curve for the rock to determine capillary pressure gradient in the direction of flow. Two-dimensional (2-D) distributions of oil and water were also imaged but only at static conditions. Images of porosity distribution in sandstones and a limestone were also obtained. Our experiences have so far proved the usefulness of nuclear magnetic resonance imaging (MRI) as a useful tool for special core analysis and identified some limitations.

INTRODUCTION

It is common practice in core flood testing to assume diffuse flow, core homogeneity and absence of capillary pressure gradients. Such assumptions cast questions over the validity of the test results but would not be necessary where MRI is used to provide information on movement and distribution of fluids inside the rock sample. Importance of capillary forces in relation to viscous forces can be assessed from the following expressions. Equations (2) derive from relationships by means of Darcy's law between flow rate of either phase and pressure drop gradient during two-phase flow.

$$\frac{\partial p_c}{\partial x} = \frac{dp_c}{dS_w} \cdot \frac{\partial S_w}{\partial x} \qquad \text{.....(1)}$$

$$\frac{\partial p_w}{\partial x} = -\frac{\frac{k k_{ro} A}{\mu_o}\frac{\partial p_c}{\partial x} - q_t}{kA(\frac{k_{ro}}{\mu_o} + \frac{k_{rw}}{\mu_w})} \qquad \text{.....(2a)}$$

and

$$\frac{\partial p_o}{\partial x} = \frac{\frac{k k_{rw} A}{\mu_w}\frac{\partial p_c}{\partial x} - q_t}{kA(\frac{k_{ro}}{\mu_o} + \frac{k_{rw}}{\mu_w})} \qquad \text{.....(2b)}$$

where, p_c - capillary pressure ($p_c = p_o - p_w$),

x - distance,

subscripts o and w denote oil and water, respectively,

k - permeability,

A - cross sectional area,

q_t - total flow rate ($q_t = (q_o + q_w)$,

μ - fluid viscosity, and

k_r - relative permeability.

The oil industry has for some decades been investigating imaging methods for visualising fluid movement and quantifying saturations in the rock sample during laboratory displacement experiments. MRI, like X-ray computer-aided tomography (CAT) scanning (Ringen and Hove, 1987; Withjack, 1987), can provide 2-D interpretation of saturation distribution in core plugs (Rothwell and Vinegar, 1985). Other imaging methods involving microwaves, VHF electrical properties, tracers in the fluid phases, radioactive sources outside the sample, X-rays and resistivity give only 1-D information about fluid distribution. MRI measures content and distribution of fluids in rocks, as well as interaction of fluids with surrounding rock matrix. The work reported in this paper demonstrates use of MRI to complement traditional core test, anlalysis and interpretation of the results.

EXPERIMENTS

A medical 120 mm horizontal bore, 0.4 Tesla NMR imaging system operating at 17.12 MHz was used to obtain all images reported here. The transmitting/receiving solenoid radio-frequency (RF) coil shown in Figure 1 was used. It has 3.8 cm internal diameter by 7.9 cm long (17 turns, 1-mm enamelled wire), and has been built with full coverage of sample length to optimise signal intensity and homogeneity of magnetic field. A sample containing hydrogen proton (^{1}H) was held in the hollow of the RF coil and was placed in the superconducting magnet of the NMR imager. The magnet was linked to an imaging console (SMIS MR2000) with software, plotter, hard disk and tape streaming facilities. Hydrogen proton signals were obtained with a two-dimensional phase encoding (2DPE) chemical shift imaging (CSI) sequence which is a modification of the spin-warp imaging sequence (Edelstein et al., 1980). The sequence generated 64 by 64 spectra for a 2-D image or 64 spectra for a 1-D image with a resolution of 0.094 cm. Acquisition and processing of the measured data were performed with the aid of a computer to produce separate images and profiles of oil and water present in the sample slice. The echo time, T_e, and the recovery time, T_R, were set at 40 ms and 3.4 s, respectively. Under these conditions about 4.5 hours or 4.5 min were required to obtain a 2-D or 1-D image across the plug length, respectively. Time constraint meant that only 1-D images were obtained at dynamic displacement conditions. A thin slice, 0.4 cm thick, parallel to the cylindrical axis of the core plug was selected for imaging. The central plane was imaged in order to minimise edge distortion

from averaging over the curvature of the plug.

The cores were outcrop Portland limestone, Clashach and Lochaline sandstones from Scotland. Core samples for only static imaging were wrapped in a thin film of waterproof material. For imaging of flow, the core samples were individually sleeved to form a flow cell. All materials used in the flow cell assembly, RF coil assembly, and waterproof film are non-magnetic, and, like the rock matrix, did not contribute to the images. A wrapped or sleeved sample was firmly mounted (no movement permitted) in the hollow of the RF coil. The flow cell is similar to a Hassler flow cell assembly. It was provided with air pressure up to 700 kPa in the annulus between sleeved core sample and case. Flexible plastic flow tubing and fittings were used to connect the inlet end of the flow cell assembly in the RF coil system to a continuous-action pump. The outlet end was connected to a pipette outside the magnet of the imager. A pressure transducer was also connected across the core using flexible plastic tubing with three-way valve fittings. During imaging the pump and the transducer were kept outside the zone of influence of the superconducting magnet because they contained magnetic components.

RESULTS AND DISCUSSION

Porosity imaging

Figure 2 shows central NMR images (in 2-D) of fully water-saturated Clashach sandstone, Lochaline sandstone and Portland limestone core plugs. NMR relaxation rates in these samples are fairly uniform, and can be explained from the mineralogical composition of these rocks given in Table 1. Table 1 also shows some properties of these rocks. The colour variations represent different amounts of water in volume elements (voxels) represented by picture elements (pixels). Each colour represents an average amount of fluid in the 0.94-$\times$ 0.94-mm by 4-mm deep voxel. The porosity distribution was obtained from proportionality of the fluid volume with the measured NMR signal data. By dividing individual voxel water content with the voxel bulk volume, the variations in water content was translated to porosity distribution as shown in the legends.

The Lochaline and Clashach sandstones are usually uniform and are generally regarded to be homogeneous. The MRI approach revealed significant non-uniformity in porosity distribution, as evidenced from the fluid distribution. These imaging experiments show that MRI can 'visualise' single fluid distribution in rocks with reasonably good resolution of 0.94 mm.

Data from the 2-D porosity interpretation for the Portland limestone provided a normal distribution as shown in Figure 3, which reveals a porosity difference spanning from about 0.02 to 0.3. In a reservoir this is one of the more common forms of the characteristic distribution of porosity. This suggests that such characteristic distribution of porosity can also be observed at the core plug scale. Figure 3 also shows a porosity profile determined with 1-D slice definition along the plane, which reveals variations from about 0.12 to 0.2 porosity units. These data indicate deviations of porosity around the bulk porosity value.

Oil/water saturation imaging

Figure 4 shows NMR signal intensity profiles from 1-D imaging, and 2-D images of water and oil jointly and fully saturating a 4-mm deep central plane of a Portland limestone core plug. Oil and water NMR linewidths in Portland limestone are very narrow, hence their joint two-peak spectrum could easily be resolved into separate spectra. The core plug, held in a flow cell made of perspex material, was initially 100% saturated with n-decane which was then flooded out with water before imaging. The images and profiles demonstrate two main features. First, the drop in water NMR signal intensity within the central part of the plane indicates poor water saturation distribution. This poor saturation distribution would not have been revealed in the 'black box' concept of core analysis. Second, the dispersed appearance of the oil NMR signal intensity indicates that the remaining oil is discontinuous. This feature provides insight into entrapment mechanism in the rock structure.

Only NMR techniques have been able to image fluid distribution in rocks with a resolution as high as 0.94 mm. Though one 4-mm deep slice only was examined in this work, multislice imaging techniques exist which can provide simultaneously a series of slice images encompassing the entire core plug. This would provide a complete insight into the *in-situ* features of the rock sample, some of which would otherwise go undetected in traditional core analysis.

Core flood imaging

Unsteady-state displacement of water by oil in a water-wet Portland limestone core plug at low velocity (3.6 cm/day) was monitored and the saturations were imaged by 1-D CSI without interrupting the flow. At such low velocity, the flow regime might be influenced by both viscous and capillary forces. The drainage displacement test was started at 100% saturation of water ($S_w = 1$), followed by

flooding with Soltrol-130 in a special flow cell. The profiles of Figure 5 show the distribution of total NMR signal from both water and oil along the central 4-mm deep plane as flooding progressed. The profile labelled 0 corresponds to image of the sample fully saturated with only water, i.e., before start of oil injection. Flooding is represented on the Figure as occurring from left to right. The profiles labelled 1 and 2, obtained in that order, indicate that Soltrol had advanced about one-third and half-way along the sample. The profile labelled 3 was obtained just before breakthrough of Soltrol at the outflow end of the core. At this stage 33% pore volume of Soltrol had been injected and none produced. Each data point on the profiles represents a pixel-averaged NMR signal, i.e., signal emitting from a small volume 4 mm by 0.94 mm by 24.4 mm (the core diameter).

The main control in imaging oil-water displacement is a balance between velocity of fluid advance and imaging speed, which depends on the imaging equipment and the sequence used. In order to achieve a balance very low flow rates were used. The range of possible flow rates can be widened with the use of fast imaging techniques in more powerful equipment. Another limitation of MRI is that in some rock-types heterogeneity of local magnetic susceptibility may not permit separate oil and water spectra to be obtained. The use of an appropriate pulse sequence and a powerful magnet may perhaps compensate such heterogeneity.

This flood imaging experiment demonstrates a method of tracking advance of displacing fluid during core flooding. Separate signal profiles of oil and water, like those shown in Figure 4, can be obtained by deconvolution of the total image. Signal intensity profiles show variations in intensity that translate to variations in fluid saturation. Where contribution to variations in intensities due to rock-fluid interaction is insignificant, as in the Portland limestone, the conversion to saturations may be based on intensity averages and corresponding material balance fluid content in the core plug.

Figure 6(a) shows a water saturation profile obtained by imaging in an unsteady state imbibition test of water displacing oil in a water-wet Portland limestone core plug (Enwere and Archer, 1992). Imbibition capillary pressure curve for the rock, obtained by porous plate method using air-brine system and scaled to the oil-water system, is shown in Figure 6(b). The smooth-line saturation profile is a fit to discrete experimental data obtained by imaging at a flood stage before breakthrough. The core water flood was conducted at very low flood rate, therefore effects of capillary forces might be significant.

By determining the gradients $\frac{\partial S_w}{\partial x}$ on the saturation profile and $\frac{dp_c}{dS_w}$ on the

capillary pressure curve at any point saturation, the capillary pressure gradient $\frac{\partial p_c}{\partial x}$ was obtained with equation (1). Corresponding phase pressure drop gradients are obtained using equations (2). Table 2 presents a comparison between the gradients. Capillary pressure gradients are difficult to quantify from conventional displacement calculations because saturation profiles are unknown. It is common practice to use high flow rates, which may not be representative of the reservoir flow conditions, in order to swamp the capillary pressure gradient.

CONCLUSIONS

NMR imaging has been used successfully in these investigations:

1. To 'visualise' distribution of oil or water in a core plug by imaging the NMR signal emited by the fluid. Since the NMR signal is proportional to the fluid content, the NMR spectrum and signal image, for a given rock-fluid relaxation parameter, reflects the fluid content and its distribution. Variation in the mineralogical (species) content and effects of confining surface of the rock limits the accuracy of determining fluid content and distribution from the NMR signal. However it is possible to measure the spatial distribution of the relaxation rates, which embodies the mineralogical and confining surface effects.

2. To provide porosity distribution within a rock sample, as evidenced from the distribution of a fluid with which the sample is completely saturated. This has indicated porosity variations within the rock samples. Porosity measured with MRI is accurate within 5%.

3. To indicate the presence and spatial positions of movable oil and water simultaneously present in a rock sample by imaging their chemical shifts. Separate images of oil and water NMR signal distributions are produced in Portland limestone samples which exhibit narrow oil and water NMR linewidths. By translating these signals in terms of oil and water contents, the saturation distribution inside the core were obtained. Part of the NMR signal (corresponding to about 200 counts) from the immovable fraction of the fluid was not measured but was obtained from extrapolation.

4. To obtain saturation profile at various stages of a core flood directly. A saturation profile has been used in conjunction with the capillary pressure curve for the rock to quantify capillary pressure gradients during the core flooding.

5. Phase pressure drop gradients have been compared with capillary pressure gradients in the direction of flow. This demonstrates the possibility of conducting displacement tests under viscous-capillary force control while taking proper

account of the effects of capillary forces, hence providing viscous-capillary force ratios. The ratios have potential for use in scaling up relative permeability data from a laboratory test to simulator-scale grid blocks.

REFERENCES

Edelstein, W. A., Hutchinson, J. M. S., Johnson, G. and Redpath, T., 1980. Spin warp NMR imaging and applications to human whole body imaging. Physics in Medicine and Biology, 25(4): 751-756.

Enwere, M. P. and Archer, J. S., 1992. NMR imaging for water/oil displacement in cores under viscous-capillary force control. Paper SPE 24166 presented at the eighth symposium on EOR held in Tulsa, Oklahoma, April 22-24.

Ringen, J. K. and Hove, A., 1987. The use of X-ray tomography in core analysis. In North Sea Oil & Gas Reservoirs. (J. Kleppe et al. Eds). Graham & Trotman, 209pp.

Rothwell, W. P. and Vinegar, H. J., 1985. Petrophysical applications of NMR imaging. Applied Optics, 24(23): 3970.

Withjack, E. M. 1987. Computed tomography for rock-property determination and fluid-flow visualisation. Paper SPE 16956 presented at the 62^{nd} Annual Technical Conference and Exhibition of the Society of Petroleum Engineers held in Dallas, Texas, September 27-30.

TABLE 1

Property and mineral composition of rocks

Rock sample :	Clashach sandstone
Type :	Aeolian sandstone
Grain size :	0.2 mm
Porosity :	19%
Permeability :	296 md
Quartz :	91%
Feldspar:	5%
Clay minerals :	trace
Shape :	sub-rounded
Sphericity :	Poor
Rock sample :	Lochaline sandstone
Type :	Shallow marine bar sand
Grain size :	0.2 mm
Porosity :	20%
Permeability :	223 md
Quartz :	95%
Clay minerals :	0
Shape :	Sub-rounded
Sphericity :	Poor
Rock sample :	Portland limestone
$CaCo_3$:	97%
Kaolinite :	2%
Calcite :	trace
Porosity :	16%
Permeability :	40 md

TABLE 2

Capillary pressure and phase pressure drop gradients
along the core behind flood front

x (cm)	S_w (PV)	$\frac{\partial p_c}{\partial x}$ (kPa/cm)	$\frac{\partial p_w}{\partial x}$ (kPa/cm)	$\frac{\partial p_o}{\partial x}$ (kPa/cm)
0.094	0.551	19.154	-5.600	13.554
0.188	0.537	19.115	-6.850	12.265
0.282	0.523	19.030	-8.089	10.941
0.376	0.520	18.899	-9.272	9.627
0.470	0.497	18.725	-10.357	8.368
0.564	0.484	18.509	-11.317	7.192
0.658	0.472	18.253	-12.133	6.120
0.752	0.460	17.957	-12.797	5.160
0.846	0.449	17.623	-13.308	4.315
0.940	0.438	17.253	-13.672	3.581
1.034	0.427	16.847	-13.897	2.950
1.128	0.417	16.408	-13.994	2.414
1.222	0.408	15.936	-13.976	1.960
1.316	0.398	15.434	-13.853	1.581
1.410	0.390	14.902	-13.637	1.265
1.504	0.381	14.342	-13.340	1.002
1.598	0.373	13.755	-12.969	0.786
1.692	0.366	13.143	-12.534	0.609
1.786	0.359	12.506	-12.043	0.463
1.880	0.352	11.847	-11.502	0.345
1.974	0.346	11.167	-10.919	0.248
2.068	0.340	10.467	-10.296	0.171

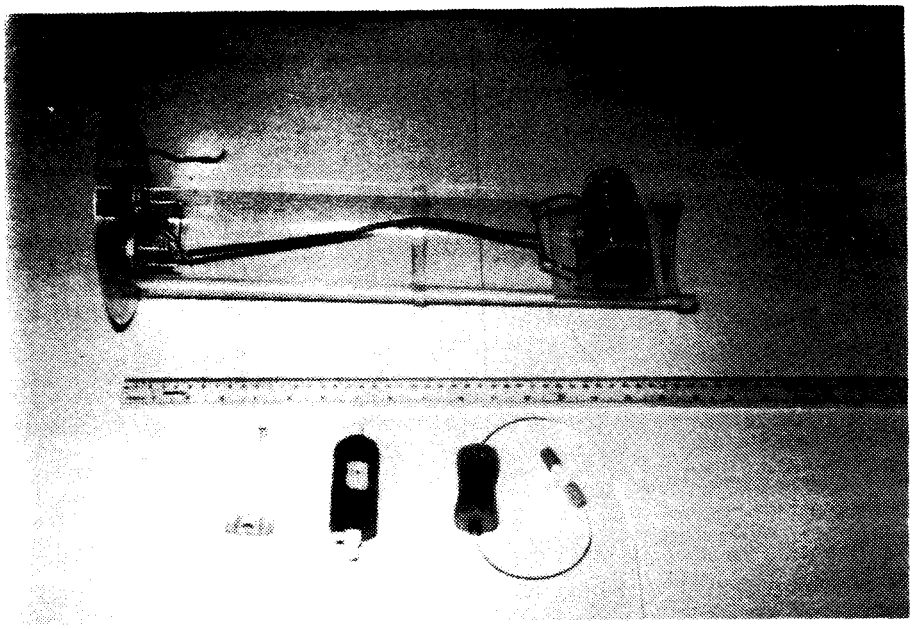

Figure 1: Transmitting/receiving RF coil.

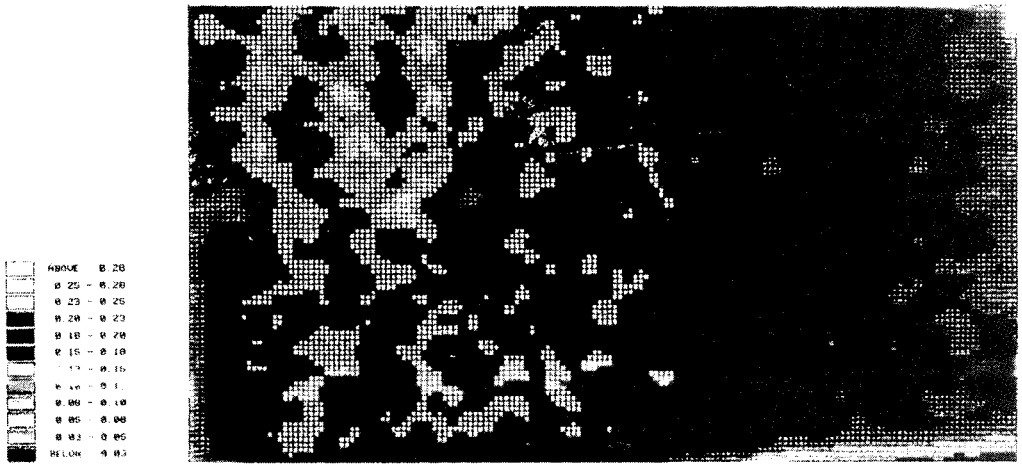

Clashach Sandstone

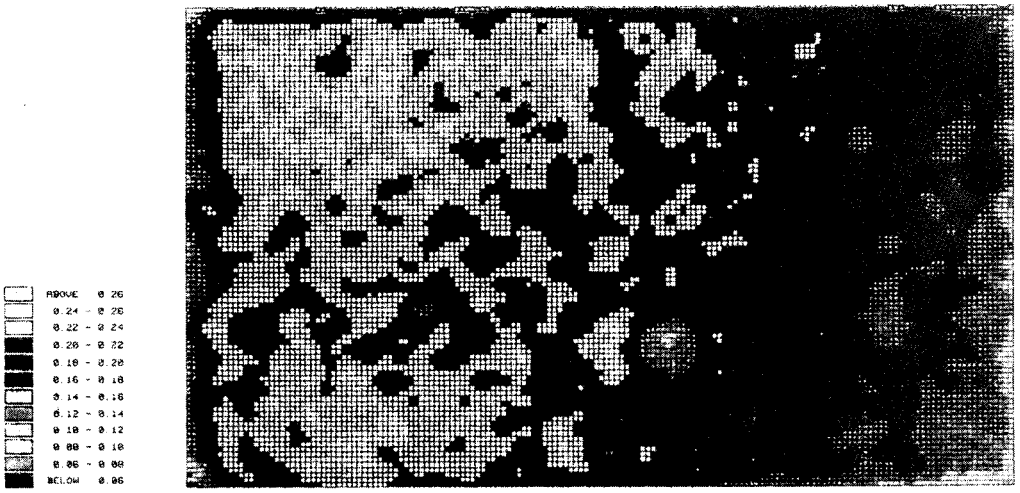

Lochaline Sandstone

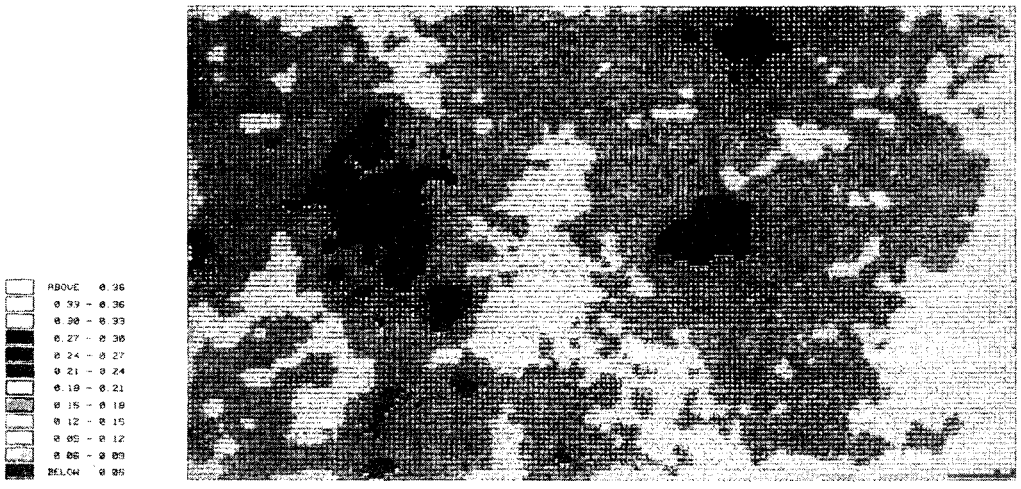

Portland Limestone

Figure 2: 2-D images of porosity distribution in 4-mm deep plane of plugs.

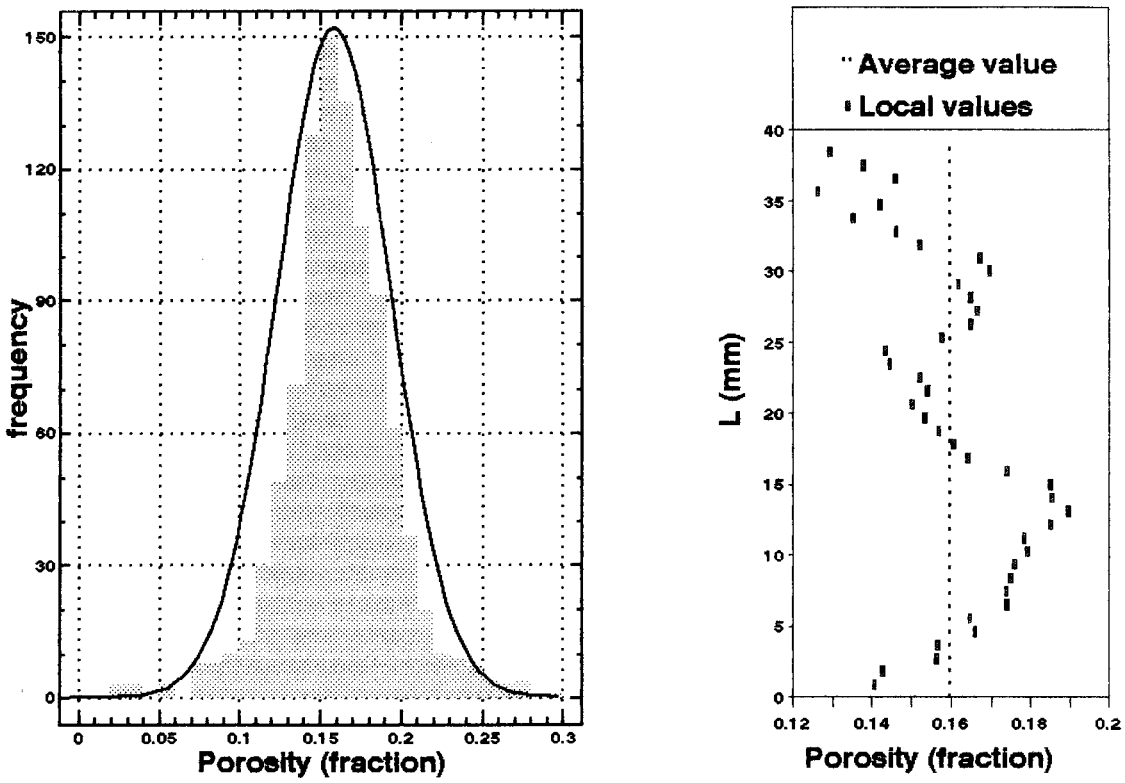

Figure 3: Porosity distribution in Portland limestone.

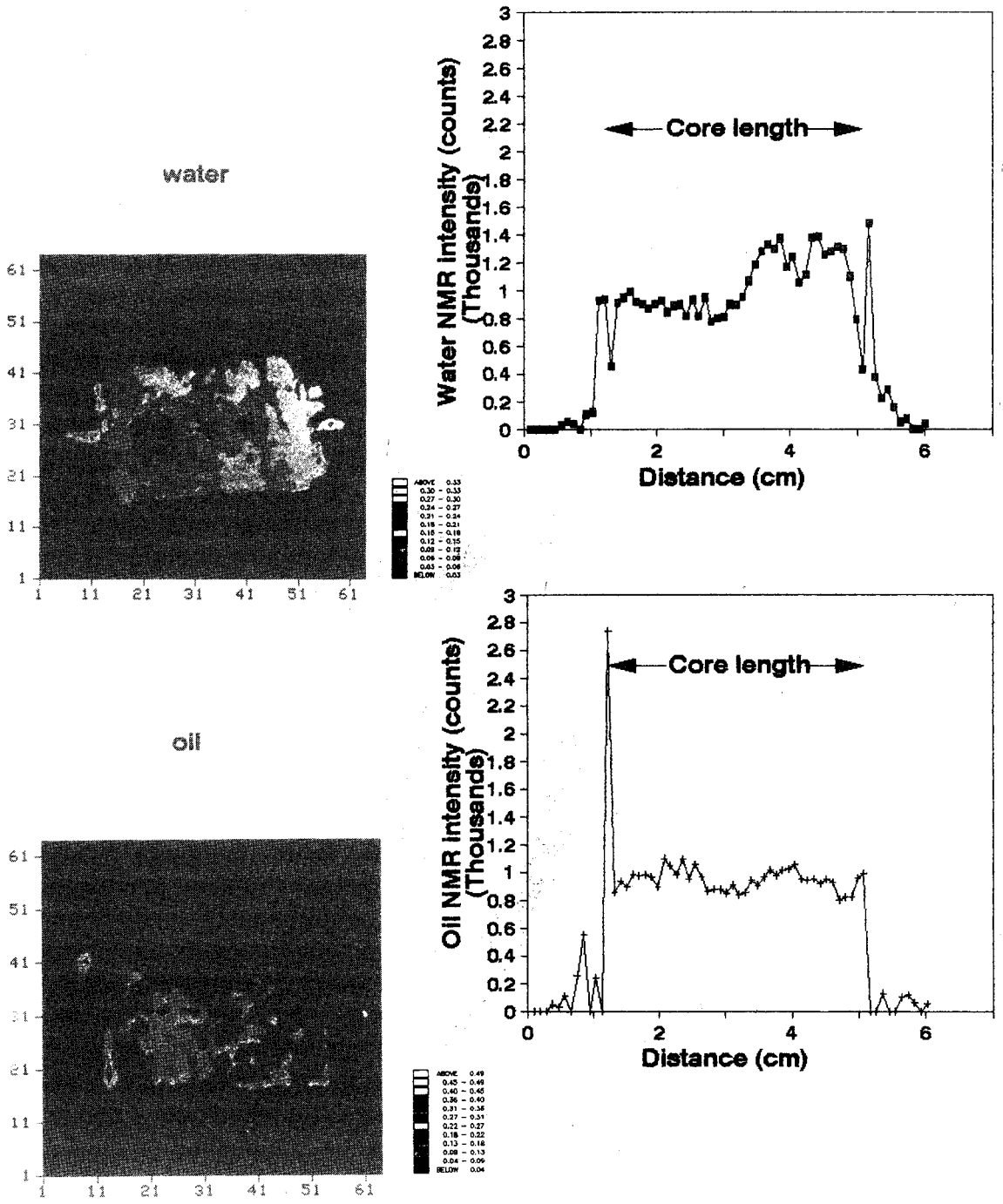

Figure 4: 2-D and 1-D distributions of fluid NMR intensities in 4-mm deep plane of Portland limestone plug.

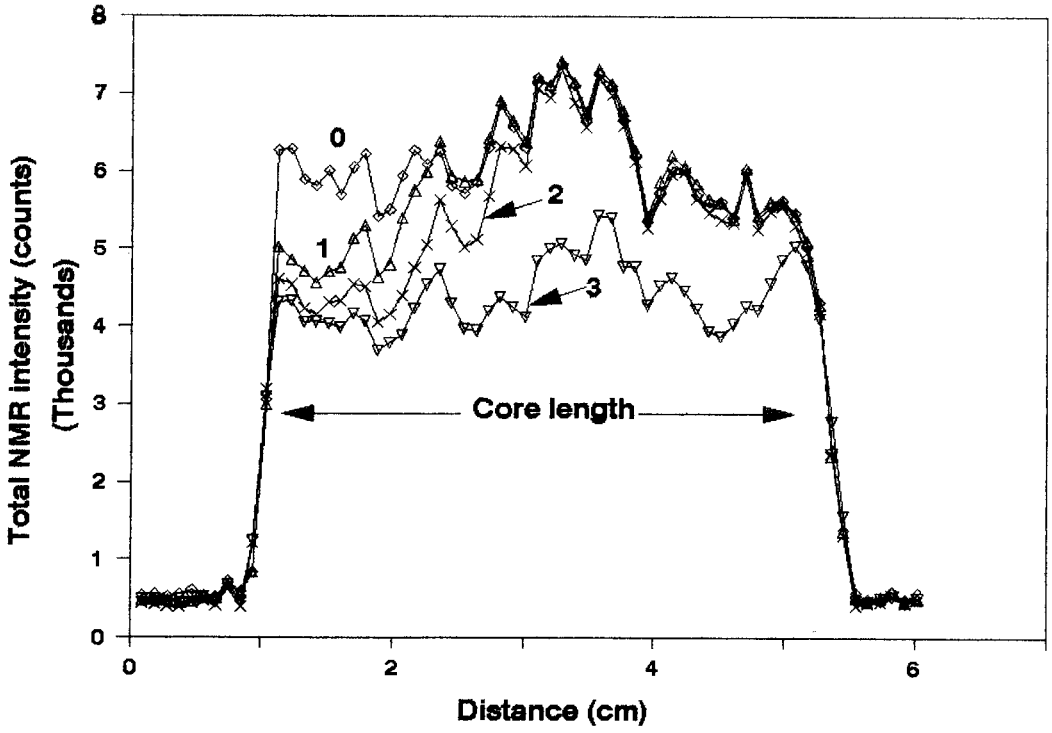

Figure 5: Combined oil-water intensity distribution in 4-mm deep plane of Portland limestone plug.

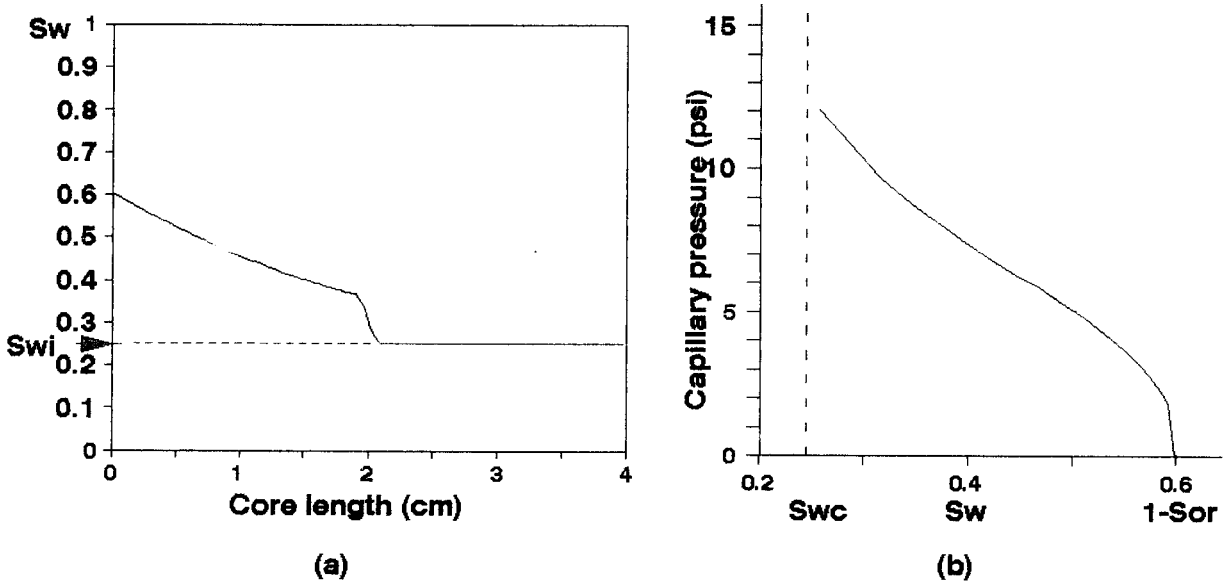

Figure 6: (a) Water saturation profile and; (b) capillary pressure function.